Resonant Mass Gravitational Wave Detectors

Noise sources and measurement of displacements

Course Project : Gravitational Waves Physics and Astronomy

Advait Mehla

Contents

1 Introduction

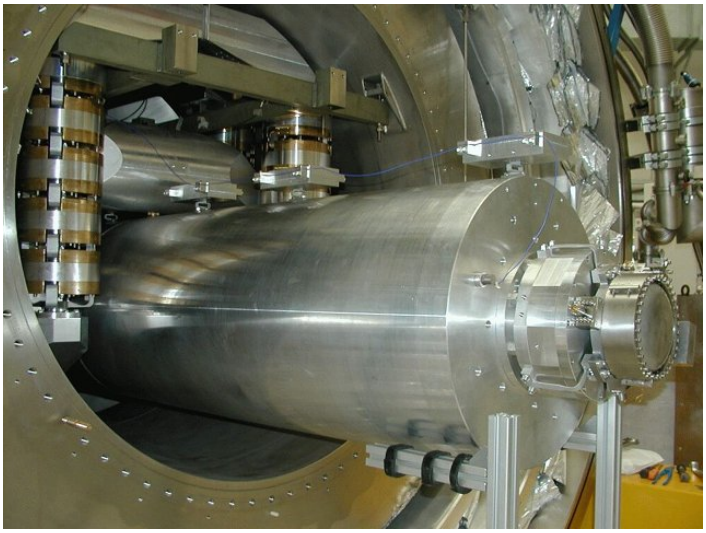

Figure 1: The AURIGA detector at Italy

The resonant bar GW detector is a precursor to modern interferometric experiments, developed by Joseph Weber in the 1960s and replicated by several other groups all over the world. They work on the idea that a GW wave passing through the bar would cause it to resonate, and even a brief burst would leave the bar 'ringing' for several minutes. Measuring these vibrations would let us detect gravitational waves.
They failed to detect any gravitational wave events as the apparatus was only sensitive to extremely loud ones, like supernovae within our own galaxy estimated to only occur a few times a century. But the instrumentation techniques that were developed for reaching extremely low sensitivities created the expertise required to make LIGO and other current missions a success.

2 Measurement Challenges

As we saw in class, for a burst with amplitude h_0, oscillations in the fundamental mode of a bar are $\xi_0 \sim Lh_0$. For a supernova in our own galaxy, an extremely rare event estimated to happen a few times every century, h_0 is *at most* of the order of 10^{-20}. To have a realistic shot at detecting even such events, we must be able to sensitive to $h_0 \sim 10^{-21}$, which gives us an oscillation amplitude of $\xi_0 \sim 3.5 \times 10^{-21}$, assuming we use one of the largest[1] Weber bars ever made, the one located at Bell Labs. This is of course, a million times smaller than the size of a proton, leading to the development ingenious methods of detection and noise control. Although these bars never led to a detection and were the subject of controversy due to the actions of their pioneer, these efforts enabled the successful interferometric gravitational wave detectors we have today. To analyse how scientific collaborations around the world designed experiments to detect displacements at such a tiny scale, we will first examine the experimental setup required for these attempts and move on to focus on the noise sources that would hinder them.
There are a few advantages to the bar setup which aid our measurements, mainly that we primarily wish to measure coherent displacements of a large surface, over which random microscopic fluctuations would cancel out. Also, intuitively, thermal noise

cannot easily generate vibrations in a large and heavy object. Additionally, while $\xi_0(t)$ appears to be prohibitively small, we only need to focus on certain frequency ranges where GWs are would make the bar resonate, and thus look for spikes in a particular frequency window of $\tilde{\xi_0}(\omega)$ and not the full frequency range. This is another fact that experimentalists have used to their advantage, as detecting such signals over the entire frequency space would be extremely daunting.

3 The double oscillator

To measure these displacements, we need to use transducers, which are devices which convert displacements to an electrical signal. Particularly, we try to use resonant transducers, which mechanically amplify the displacements in question before converting them to signals. Resonant transducers involve coupling the bar with another oscillator that has a light mass. To model this system, we can assume an oscillator with effective mass $m_0 (= M/2$ for resonant bars) and frequency ω_0 to be coupled to another oscillator with effective mass and frequency of m_t and ω_t. Figure 1 shows a schematic diagram of such an oscillator, with displacements of the bar and transducer from their respective equilibrium positions given by $\xi_0(t)$ and $\xi_t(t)$. To analyse the

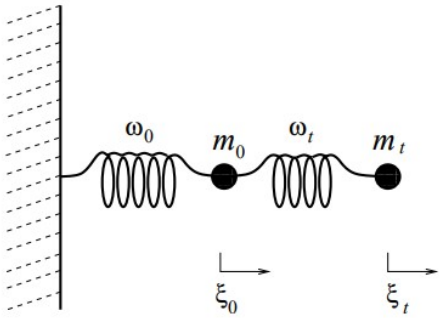

Figure 2: Schematic diagram of a double oscillator [2]

dynamics of this system(initially without considering dissipation effects), we look at its Lagrangian-

$$L = \frac{1}{2} m_0 \dot{\xi_0^2} + \frac{1}{2} m_\mathrm{t} \dot{\xi_\mathrm{t}^2} - V\left(\xi_0, \xi_\mathrm{t}\right) \tag{1}$$

where,

$$V\left(\xi_0, \xi_\mathrm{t}\right) = \frac{1}{2} m_0 \omega_0^2 \xi_0^2 + \frac{1}{2} m_\mathrm{t} \omega_\mathrm{t}^2 \left(\xi_\mathrm{t} - \xi_0\right)^2 \tag{2}$$

Defining $\mu = m_t/m_0$, and assuming external(due to GWs) forces $F_0(t)$ and $F_\mathrm{t}(t)$ acting on the masses we get,

$$\ddot{\xi_0} + \omega_0^2 \xi_0 + \mu \omega_\mathrm{t}^2 \left(\xi_0 - \xi_\mathrm{t}\right) = \frac{F_0(t)}{m_0} \tag{3}$$

$$\ddot{\xi_\mathrm{t}} + \omega_\mathrm{t}^2 \left(\xi_\mathrm{t} - \xi_0\right) = \frac{F_\mathrm{t}(t)}{m_\mathrm{t}} \tag{4}$$

We can find the response of this system to an impulsive force on the bar, like that imparted by a GW burst. Due to its low mass, this would not affect the transducer.

Thus, we can set $F_0/m_0 = a_0\delta(t)$ and $F_\mathrm{t} = 0$ and solve this system in the Fourier domain, obtaining

$$\tilde{\xi_0}(\omega) = a_0 \frac{-\omega^2 + \omega_\mathrm{t}^2}{(\omega^2 - \omega_+^2)\,(\omega^2 - \omega_-^2)}, \tag{5}$$

$$\tilde{\xi_t}(\omega) = a_0 \frac{\omega_\mathrm{t}^2}{(\omega^2 - \omega_+^2)\,(\omega^2 - \omega_-^2)} \tag{6}$$

where $\omega_\pm^2$ are the two resonant frequencies, which are the roots of

$$\omega^4 - (\omega_0^2 + (1+\mu)\omega_t^2)\omega^2 + \omega_0^2\omega_t^2 = 0 \tag{7}$$

For a resonant transducer, $\mu << 1$ leads to $\omega_\pm \approx \omega_0\left(1 \pm \mu/\sqrt{2} + O(\mu)\right)$
We can evaluate the Fourier transform of equations 21 and 6 by including all four poles for $t > 0$ after some analysis and applying Cauchy theorem. This gives us

$$\xi_0(t) \simeq \frac{a_0}{\omega_0} \sin\omega_0 t \cos\omega_b t \tag{8}$$

$$\xi_\mathrm{t}(t) \simeq -\frac{a_0}{\omega_0\sqrt{\mu}} \cos\omega_0 t \sin\omega_b t \tag{9}$$

Where $\omega_b = 0.5 \cdot \omega_0\sqrt{\mu} << \omega_0$ is the beat frequency.

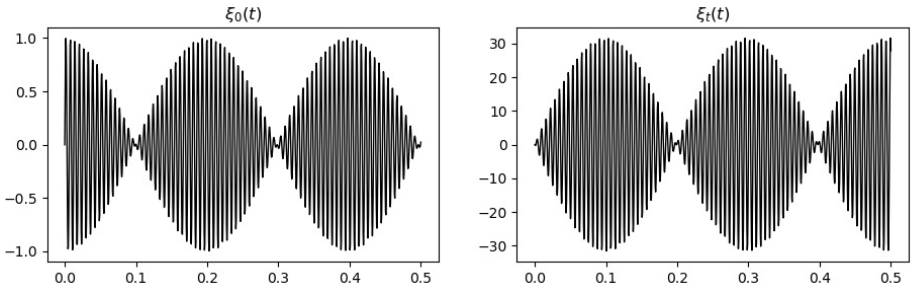

Figure 3: Displacements of the bar and transducer for $\mu = 10^{-3}$

From the plots above, we can see how energy flows periodically between the bar and transducer. Evidently, the amplitude of displacement in the transducer is significantly larger than that of the bar, leading to a mechanical amplification with a gain of $1/\sqrt{\mu}$. Lower values of m_t are thus favourable, but masses that are too light are subjected to high levels of thermal noise.
Introducing dissipation in this system, the following equations replace 3 and 4

$$m_0\left[\ddot{\xi}_0 + \omega_0^2\xi_0 + \mu\omega_\mathrm{t}^2\left(\xi_0 - \xi_\mathrm{t}\right)\right] = F_0 + f_0^\mathrm{diss}\,, \tag{10}$$

$$m_\mathrm{t}\left[\ddot{\xi}_\mathrm{t} + \omega_\mathrm{t}^2\left(\xi_\mathrm{t} - \xi_0\right)\right] = F_\mathrm{t} + f_\mathrm{t}^\mathrm{diss}\,, \tag{11}$$

where, dissipative forces f_0^diss , $f_\mathrm{t}^\mathrm{diss}$ are

$$f_0^\mathrm{diss} = -m_0\gamma_0\dot{\xi}_0 - m_\mathrm{t}\gamma_\mathrm{t}\left(\dot{\xi}_0 - \dot{\xi}_\mathrm{t}\right), \tag{12}$$

$$f_\mathrm{t}^\mathrm{diss} = -m_\mathrm{t}\gamma_\mathrm{t}\left(\dot{\xi}_\mathrm{t} - \dot{\xi}_0\right), \tag{13}$$

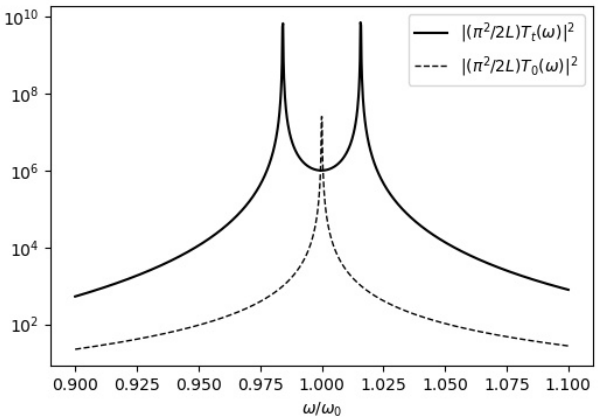

Figure 4: The squared moduli of transfer functions of bar and transducer

Here γ_0 and γ_t are related to the quality factors of the bar and transducer by $Q_0 = \omega_0/\gamma_0$ and $Q_t = \omega_t/\gamma_t$. The Fourier domain solution for the modified differential equations comes out to be

$$\tilde{\xi}_t(\omega) = \frac{\left(\tilde{F}_0(\omega)/m_0\right)\omega_0^2 - \left(\tilde{F}_t(\omega)/m_t\right)(\omega^2 - \omega_0^2 + i\omega\gamma_0)}{(\omega^2 - \omega_+^2 + i\omega\bar{\gamma})\,(\omega^2 - \omega_-^2 + i\omega\bar{\gamma})} \tag{14}$$

Since we are only interested in the effects of GWs on this system, we can set $\tilde{F}_0(\omega) = -(2L/\pi^2)\,m_0\omega^2\tilde{h}(\omega)$ and $\tilde{F}_t(\omega) = 0$. After doing this, we can obtain a transfer function for the transducer's response to a GW

$$T_t(\omega) = -\frac{2L}{\pi^2}\frac{\omega_0^2\omega^2}{(\omega^2 - \omega_+^2 + i\omega\bar{\gamma})\,(\omega^2 - \omega_-^2 + i\omega\bar{\gamma})} \tag{15}$$

where $\bar{\gamma} = (\gamma_0 + \gamma_t)/2$. This quantity determines the extent of dissipation, and we can then define an overall mechanical quality factor of this system by $\bar{\gamma} = \omega_0/Q_m$ so that $2/Q_m = (1/Q_0 + 1/Q_t)$. Q_m typically reaches values on the order of 10^6. The two peak values of the transducer transfer function are much higher than that of the bar alone. This transfer function has been visualised in Figure 4.

4 The resonant transducer

After the double oscillator amplifies the displacement, it must be next readout by transforming it to an electrical signal. Transducers generally use the small displacements to modulate a stored electromagnetic field. Commonly used for this purpose are capacitive transducers, where one plate of the capacitor is the light mass itself while the other is rigidly supported by the large mass.

The electrical signal produced by this transducer is still quite low and must be amplified. A SQUID(Superconducting QUantum Interference Device) is the ideal amplifier for this task at cryogenic temperatures. However, the large output impedance($\sim 10^5\Omega$) of the transducer must be matched with the small input impedance($\sim 10^{-2}\Omega$) of the SQUID, and a transformer is used for this. This acts as an LC circuit, making the bar+transducer+circuit system a triple oscillator. This is very complicated to analyse, but we can qualitatively understand things by figuring out the coupling of the transducer and the electric oscillator, as we did before for the double oscillator.

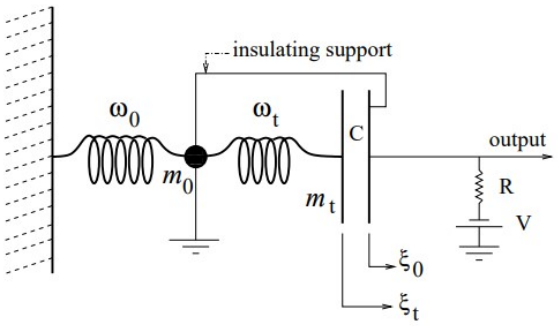

Figure 5: Schematic diagram of a capacitive transducer [2]

We note that the output of the transducer, V depends linearly on the displacement $\xi_{\rm t}$. In the Fourier domain, this can be written as $\tilde{V}(\omega) = \alpha\tilde{\xi}_{\rm t}$. Here we approximate $\alpha(\omega) \sim i\omega$ to be roughly constant over the small frequency range of interest, and pick its value at ω_0. This gives us

$$V(t) = Z_{21}\dot{\xi}(t) \tag{16}$$

where $Z_{21} = \alpha/(-i\omega_0)$. Now, the ratio of EM and elastic energies gives us a measure of energy transfer between the transducer and the LC oscillator

$$\beta \equiv \frac{E_{\rm em}}{E_{\rm elas}} = \frac{C\alpha^2}{m_{\rm t}\omega_0^2} = \frac{\alpha^2}{m_{\rm t}\omega_0^3|Z|} \tag{17}$$

This equation helps illustrate the advantage of the resonant inducer, as β is inversely proportional to m_t as we can see. If instead this readout system would directly be coupled to the bar, it would be m_0 in the denominator which is orders of magnitude larger. The resonant transducer thus plays the role of a mechanical transformer, coupling the high mechanical output impedance of the bar with low mechanical input impedance of the capacitor.
The best coupling between the electrical and mechanical modes occurs when $\omega_{em} = \omega_0$, when the entire system is in resonance. But one issue with this is that Q_{em} is usually much lower than 10^6 and it is a challenge to increase this number for electrical oscillators. The alternative is to detune ω_{em} and set it to about 30% higher than the two mechanical modes. This ensures that only a fraction of the energy is transferred to the electrical mode, where it dissipates quickly. However, this method reduces the bandwidth, as a lower β implies a smaller bandwidth.
Now that the displacement is encoded as an electric signal, it can be amplified using SQUIDs and readout. Using this scheme, it has been possible to measure infinitesimal changes of energy equivalent to the absorption of just $O(100)$ quanta of ω_0, or $\Delta E \sim 100\hbar\omega_0$. This means we can detect vibrations corresponding to around a 100 phonons in a multi-ton object!

5 Noise Sources

In order to characterise different noise sources, we can look at two different metrics:

1. The minimum detectable energy deposited by a GW in order to overcome the noise

2. The contribution of the component to the noise spectral density

The output of the detector can be written in the form $s(t) = h(t) + n(t)$, where $h(t)$ is caused by GWs and $n(t)$ is due to noise. We have already seen that when GWs are the only force acting on the bar, the corresponding displacement is given by $\tilde{\xi}^{(h)} = T(\omega)\tilde{h}(\omega)$. Additionally, noise will give further contributions to the displacement given by $\tilde{\xi}^{(n)} = T(\omega)\tilde{n}(\omega)$.
The noise spectral density $S_n(\omega)$ is related to the spectral density of the displacement caused by that noise by

$$S_\xi^{\text{noise}} = |T(\omega)|^2 S_n(\omega), \tag{18}$$

Where the spectral density of displacement is given by

$$\left\langle \xi^2(t) \right\rangle = \int_0^\infty \frac{d\omega}{2\pi} S_\xi(\omega) \tag{19}$$

Therefore, to compute the contribution to $S_n(\omega)$ due to a given noise source, say thermal noise, we can compute the spectral density of the displacement induced by this noise, and we then divide it by $|T(\omega)|^2$.

5.1 Thermal Noise

Thermal noise is due to the kinetic energy of the atoms of the detector. Intuitively, the minimum detectable excitation in the presence of thermal noise for a bar at temperature T should be

$$\Delta E \approx kT$$

But this is not the case in high-Q mechanical oscillators, as shown by Weber, and the figure is in fact much smaller. Here is an intuitive explanation of the same - since the relaxation time τ_0 for the fundamental mode of the bar is ~ 10 min, the time needed to cause fluctuations on the order of kT will also be $\sim \tau_0$.
Therefore, if we sample the the state of the bar with time resolution Δt, the minimum GW energy detectable against the thermal noise would actually be

$$\left(\Delta E_{\text{min}}\right)_{\text{thermal}} \simeq kT \frac{\Delta t}{\tau_0}, \tag{20}$$

This is valid as long as $\Delta t \geq \tau_g$, the timescale of the GW burst itself. This result can also be derived by modelling the thermal noise by a stochastic force, the Nyquist force. The full derivation involves statistical mechanics and is beyond the scope of this report. The fluctuation-dissipation theorem states that for any linear system subjected to an external force $F(t)$ and having a velocity of $v(t) = \dot{x}(t)$, the equation of motion in the Fourier domain can always be written as

$$\tilde{F}(\omega) = Z(\omega)\tilde{v}(\omega) \tag{21}$$

This gives us an expression for $S_F(\omega)$, the power spectrum of the force responsible for causing thermal noise

$$S_F(\omega) = 4kT \,\text{Re}\, Z(\omega) \tag{22}$$

For a damped harmonic oscillator, Z is given by

$$Z = -\frac{im_0}{\omega}\left(\omega^2 - \omega_0^2 + i\gamma_0\omega\right), \tag{23}$$

$$\text{Re}\; Z = m_0\gamma_0 \tag{24}$$

We can now determine the noise spectral density due to thermal fluctuations considering the bar mode ξ_0. Taking $\tilde{v}(\omega) = -i\omega\tilde{\xi}_0(\omega)$, Equation 21 gives us

$$\tilde{\xi}_0(\omega) = \frac{1}{-i\omega Z(\omega)}\tilde{F}(\omega) \tag{25}$$

Thus,

$$S_\xi^{\text{thermal}}(\omega) = \frac{1}{\omega^2|Z(\omega)|^2}S_F(\omega) \tag{26}$$

$$= \frac{4kTm\gamma_0}{\omega^2|Z(\omega)|^2}. \tag{27}$$

We can further substitute $Z(\omega)$ in terms of the transfer function of ξ_0 to obtain

$$S_\xi^{\text{thermal}}(\omega) = \frac{4kT\gamma_0}{m_0\omega^4}\left(\frac{\pi^2}{2L}\right)^2|T_0(\omega)|^2 \tag{28}$$

Now, we finally get the noise spectral density due to the thermal noise using Equation 18 as

$$S_n^{\text{thermal}}(f) = \frac{\pi}{Q_0}\frac{kT}{Mv_s^2}\frac{f_0^3}{f^4} \tag{29}$$

After substituting $m_0 = M/2$, $L = \pi v_s/\omega_0$ and $\gamma_0 = \omega_0 Q_0$.
Note that $S_n(f)$ shows no distinct behaviour around the fundamental frequency f_0, and instead has a smooth frequency dependence going as f^{-4}. This implies that if thermal noise was the only source of noise, bars would be wideband instruments. We will see that bars show narrowband behaviour only after incorporating read-out noise. This equation also shows the importance of having a high quality factor.
If we repeat the same analysis including the complete bar-transducer system, the total noise spectral density comes out to be

$$S_n^{\text{thermal}}(f) = S_n^{\text{thermal,bar}}(f) + S_n^{\text{thermal,trans}}(f) \tag{30}$$

$$= \pi\frac{kT}{Mv_s^2}\frac{f_0^3}{f^4}\left[\frac{1}{Q_0} + \frac{1}{\mu Q_{\text{t}}}\frac{\left(f^2 - f_0^2\right)^2 + \left(ff_0/Q_0\right)^2}{f_0^4}\right]$$

$$\approx \pi\frac{kT}{Mv_s^2}\frac{f_0^3}{f^4}\left[\frac{1}{Q_0} + \frac{1}{\mu Q_{\text{t}}}\frac{\left(f^2 - f_0^2\right)^2}{f_0^4}\right] \tag{31}$$

We see that this is a sum of the term we derived for the bar alone with a new term representing the coupling. The first term inside the bracket is identical to the one in Equation 29. The term ff_0/Q^2 is negligible throughout the frequency range and can be ignored. The total noise spectral density along with its components has been plotted in Figure 6.
We observe that the transducer component disappears at $f = f_0$ but becomes important as we go away from the fundamental frequency. The noise profile is also minimum at f_0 rather than the fundamental modes $f_\pm$.

5.2 Readout Noise

The next crucial noise component to consider is the noise introduced by the readout scheme. The output of the capacitive transducer is a voltage V, but this needs to be

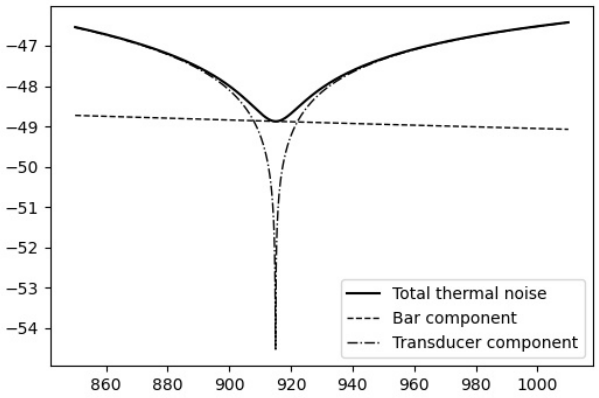

Figure 6: Log of the components of thermal noise spectral density for the numerical values $Q_0 = Q_t = 2 \times 10^6$, $T = 1$ K, $M = 2300$ kg, $L = 3$ m, $v_s = 5400$ m/s, $f_0 = 915$ Hz, $\mu = 2.4 \times 10^{-4}$

amplified further to be digitised and recorded. The amplifier would have an associated wideband noise that can be described by the spectral density of the output potential, S_V. This can be taken to be approximately constant in the frequency range of interest. As $V = \alpha\xi_t$, any error in measurement of V due to electronic noise would result in a perceived error in ξ_t. This can be described by spectral density of the displacement

$$S_{\xi_\mathrm{t}}^{\mathrm{ampl}} = \frac{1}{\alpha^2} S_V \tag{32}$$

As both α and S_V are nearly constant, $S_{\xi_\mathrm{t}}^{\mathrm{ampl}}$ is approximately a white noise.
In order to quantitatively characterise this noise, we can again look at the energetic and spectral features like we did for thermal noise. As before, a sampling time of Δt will give a bandwidth $\Delta f \approx 1/\Delta t$. Then, the fluctuations in ξ_t^2 are given by

$$\left\langle \xi_\mathrm{t}^2(t) \right\rangle = \int_{f_0 - \Delta f/2}^{f_0 + \Delta f/2} df\, S_{\xi_\mathrm{t}}^{\mathrm{ampl}} = S_{\xi_\mathrm{t}}^{\mathrm{ampl}} \Delta f \tag{33}$$

The minimum detectable energy is therefore given by

$$\left(\Delta E_{\mathrm{min}}\right)_{\mathrm{ampl}} = m_\mathrm{t}\omega_0^2 \left\langle \xi_\mathrm{t}^2(t) \right\rangle \simeq m_\mathrm{t}\omega_0^2 S_{\xi_\mathrm{t}}^{\mathrm{ampl}} \frac{1}{\Delta t} \tag{34}$$

We see that this is inversely proportional to Δt. This can be explained by the fact that when the sampling time is small, bandwidth is large, causing the amplifier noise to flood the output. Recall also that in the case of thermal noise we saw a MDE proportional to Δt. This implies that there must be an optimal sampling time to optimise the overall MDE.
We can now proceed to look at the amplifier noise in terms of its spectral density, $S_n^{\mathrm{ampl}}(f)$. As before, we must find $S_t^{\mathrm{ampl}}(f)$ and divide it by $|T_t(\omega)|^2$.
This gives us

$$S_n^{\mathrm{ampl}}\,(f) = \mathcal{A} \frac{\left[\left(f^2 - f_+^2\right)^2 + \left(f f_0/Q_m\right)^2\right]\left[\left(f^2 - f_-^2\right)^2 + \left(f f_0/Q_m\right)^2\right]}{f^4 f_0^4} \tag{35}$$

Where $\mathcal{A} = \frac{\pi^4}{4L^2} S_{\xi_\mathrm{t}}^{\mathrm{ampl}}$. This has been plotted below. We see that the amplifier noise is minimum at $f_\pm$, unlike thermal noise.

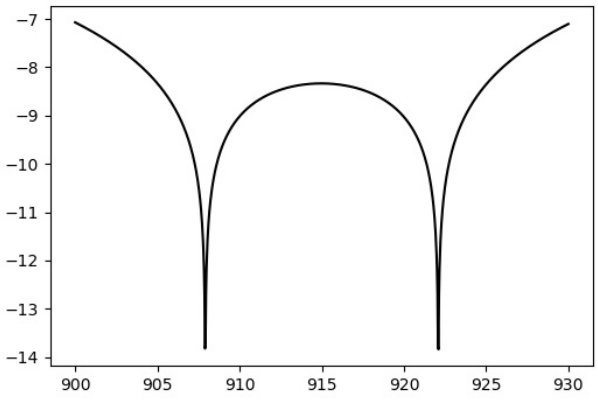

Figure 7: $\log_{10}\left[S_n^{\text{ampl}}\,(f)/\mathcal{A}\right]^{1/2}$ vs. frequency

5.3 Combining the Noises

We must now combine the aspects of both noise sources in order to get an overall view of how noise impacts resonant bars. The minimum detectable energy comes out to be

$$\Delta E_{\min} \sim kT\frac{\Delta t}{\tau} + m_{\text{t}}\omega_0^2 S_{\xi_{\text{t}}}^{\text{ampl}}\frac{1}{\Delta t} \tag{36}$$

We can minimise this to give an optimal value of Δt, which in turn yields a useful bandwidth for this system. We can take the overall relaxation time of all three modes to be $\tau = Q/\omega_0$, where Q is the overall quality factor.

$$\Delta f \simeq \frac{1}{(\Delta t)_{\text{opt}}} \sim \pi\frac{f_0}{Q}\Gamma^{-1/2} \tag{37}$$

where

$$\Gamma = \frac{m_{\text{t}}\omega_0^3 S_{\xi_{\text{t}}}^{\text{ampl}}}{4QkT}$$

With typical values, of $Q \sim 10^6$, $\Gamma \sim O(10^{-8} - 10^{-9})$, this gives us a useful bandwidth $\Delta f = O(10 - 100)Hz$. The useful bandwidth is solely determined by the noise characteristics, and has nothing to do with the resonance peak in the transfer function. At $\Delta t = (\Delta t)_{opt}$, we get

$$\Delta E_{\min} \sim 2kT\frac{(\Delta t)_{\text{opt}}}{\tau} \tag{38}$$

This can be written as

$$\Delta E_{\min} = kT_{\text{eff}} \tag{39}$$

With an effective temperature T_{eff} given by

$$T_{\text{eff}} \sim \frac{4\pi}{Q}\frac{f_0}{\Delta f}T \simeq 4\Gamma^{1/2}T \tag{40}$$

For typical values, this turns out to give $T_{\text{eff}} \approx 2\text{mK}$. This means that even with the bar at a temperature of 2K, we can detect bursts that deposit an energy equivalent to merely a few mK.

Next, we consider the total noise spectral density

$$S_n(f) = \frac{\pi k T}{M v_s^2 f_0} \left\{ \frac{f_0^4}{f^4} \left[\frac{1}{Q_0} + \frac{1}{\mu Q_t} \frac{\left(f^2 - f_0^2\right)^2}{f_0^4} \right] + \frac{Q\Gamma}{\mu} \frac{\left[\left(f^2 - f_+^2\right)^2 + \left(f f_0/Q_m\right)^2\right] \left[\left(f^2 - f_-^2\right)^2 + \left(f f_0/Q_m\right)^2\right]}{f^4 f_0^4} \right\} \tag{41}$$

Here, for given values of the quality factors and μ, the factor Γ determines the relative importance of thermal and readout noise. This therefore also controls the bandwidth Δf. We can see plots of the total noise spectral density for different values of Γ in Figure 8.

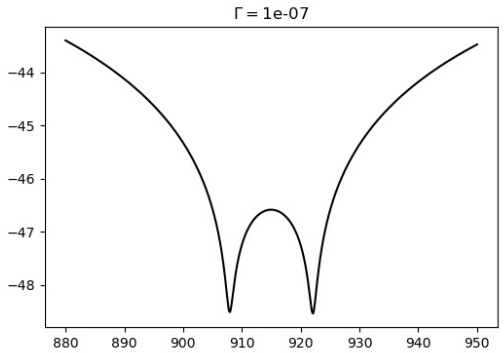

(a) Amplifier noise dominates

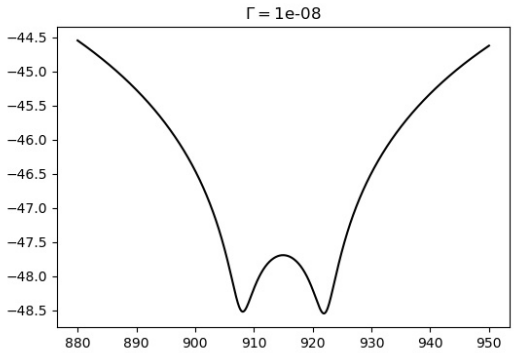

(b) Both noises comparable

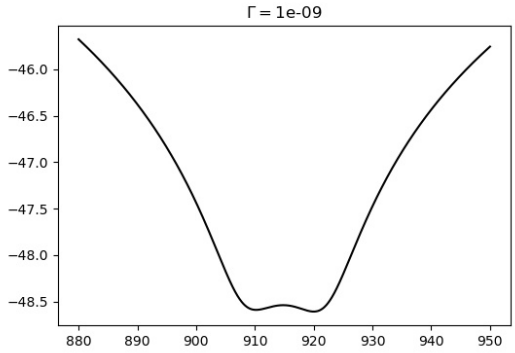

(c) Thermal noise dominates(transducer too light)

Figure 8: Total noise for different values of Γ

This curve is quite similar to the strain sensitivity plot of resonant bar detectors. Below is the observed strain sensitivity for the AURIGA detector, as of 2004.

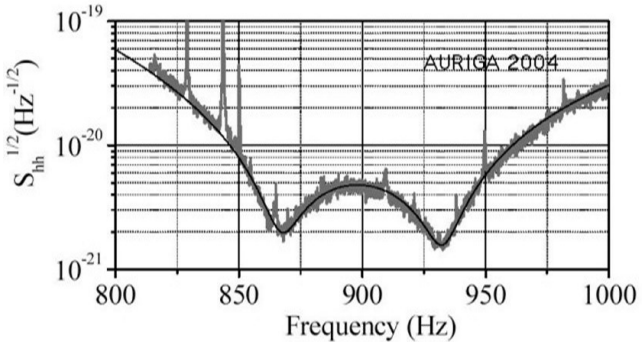

Figure 9: Image credit : [3]

6 Conclusion

In this report, I have given a complete overview of the prevalent measurement techniques used in resonant bar gravitational wave detectors, along with the noise considerations involved. This is however, just a surface level overview of this vast topic. Quantum effects also come into play and serve as an additional noise component, but these play a relatively small role in resonant detectors compared to the thermal and electronic noise. These do play an important in interferometric detectors.
Over decades of research in this field, several alternate detector schemes also emerged. These include dual spherical detectors, which were proposed to utilise an optical readout system, like a Fabry-Perot cavities which are extensively used in detectors of today. A lot of these ideas were promising but could not be brought to fruition due to issues in practicality. Interferometric detectors ultimately dominated the field and have proved to be exceptionally good at detecting GWs and are continually getting better. Although several bar detectors have been shut down as a result of this, some of them are still active, with efforts to cross-correlate signals with LIGO and proposals to use them as probes of quantum gravity and dark matter.

References

[1] Odylio Denys Aguiar. Past, present and future of the resonant-mass gravitational wave detectors. *Research in Astronomy and Astrophysics*, 11(1):1, Jan 2011.

[2] Michele Maggiore. *Gravitational Waves. Vol. 1: Theory and Experiments*. Oxford Master Series in Physics. Oxford University Press, 2007.

[3] Francesco Ronga. Detection of gravitational waves with resonant antennas. *Journal of Physics: Conference Series*, 39(1):18, may 2006.